

Supplementary Information for

**Optimization of Crystal Packing in Semiconducting Spin-Crossover Materials with Fractionally Charged TCNQ $^{\delta-}$  Anions ( $0 < \delta < 1$ )**

Ökten Üngör,<sup>a</sup> Eun Sang Choi,<sup>b</sup> Michael Shatruk<sup>a,b,\*</sup>

<sup>a</sup> Department of Chemistry and Biochemistry, Florida State University, 95 Chieftan Way, Tallahassee, FL 32306, USA

<sup>b</sup> National High Magnetic Field Laboratory, 1800 E Paul Dirac Dr, Tallahassee, FL 32310, USA

\* Corresponding author: [mshatruk@fsu.edu](mailto:mshatruk@fsu.edu)

**Contents:**

<b>Figure S1.</b> Thermogravimetric curves of solvated and desolvated forms of <b>1</b> and <b>2</b> .....	S2
<b>Figure S2.</b> Thermogravimetric curves of <b>4</b> and <b>5</b> and their desolvated forms.....	S2
<b>Table S1.</b> Data collection and crystal structure refinement parameters for <b>1·5MeCN</b> , <b>2·3MeCN</b> , and <b>2</b> .....	S3
<b>Table S2.</b> Data collection and crystal structure refinement parameters for <b>3</b> , <b>4</b> and <b>5</b> .....	S4
<b>Figure S3.</b> The asymmetric unit and crystal packing of <b>1·5MeCN</b> .....	S5
<b>Figure S4.</b> Powder X-ray diffraction pattern of <b>1</b> obtained by desolvation of <b>1·5MeCN</b> .....	S5
<b>Figure S5.</b> The overlap modes of TCNQ units in <b>1·5MeCN</b> .....	S5
<b>Table S3.</b> The charges ( $\delta$ ) of four different TCNQ $^{\delta-}$ species in <b>1a</b> , <b>2a</b> and <b>2b</b> estimated from the Kistenmacher empirical formula.....	S6
<b>Table S4.</b> The charges ( $\delta$ ) of four different TCNQ $^{\delta-}$ species in <b>3</b> and <b>4</b> estimated from Kistenmacher empirical formula.....	S6
<b>Figure S6.</b> The asymmetric unit of <b>2·3MeCN</b> .....	S7
<b>Figure S7.</b> The crystal packing of <b>2·3MeCN</b> (a) and <b>2</b> (b) viewed down the stacks of (TCNQ) $_{2}^{2-}$ dimers....	S7
<b>Figure S8.</b> The asymmetric unit of <b>3</b> .....	S7
<b>Figure S9.</b> The asymmetric unit of <b>4</b> .....	S8
<b>Figure S10.</b> The asymmetric unit of <b>5</b> .....	S8
<b>Figure S11.</b> The temperature dependence of $\chi T$ measured on the sample of <b>1·5MeCN</b> kept in the magnetometer chamber for 1 h prior to the measurement .....	S9
<b>Figure S12.</b> Thermogravimetric curve of the sample <b>1·5MeCN</b> subjected to two cooling-heating cycles between 350 and 5 K inside the magnetometer chamber .....	S9
<b>Figure S13.</b> Temperature dependence of $\chi$ measured for samples <b>4</b> and <b>5</b> between 300 and 400 K.....	S10

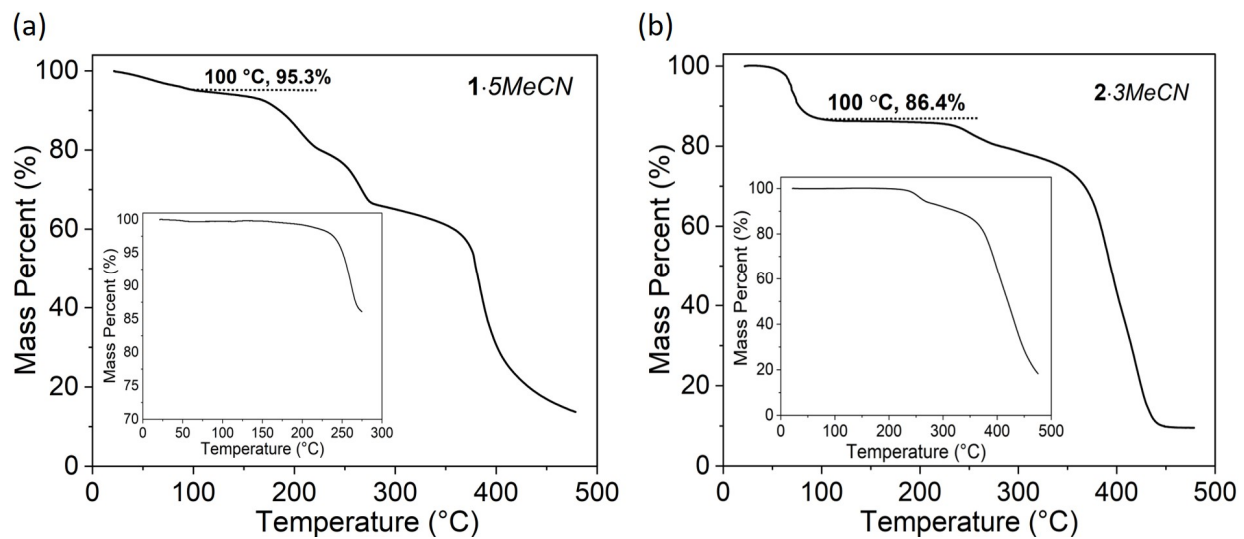


**Figure S1.** Thermogravimetric curves of the solvated and desolvated (inset) forms of **1** and **2**. The mass loss of 4.7% reached at 100 °C for **1** and 13.6% reached at 100 °C for **2** corresponds to the loss of ~1.5 MeCN molecules and ~3 MeCN molecules per formula unit, respectively.

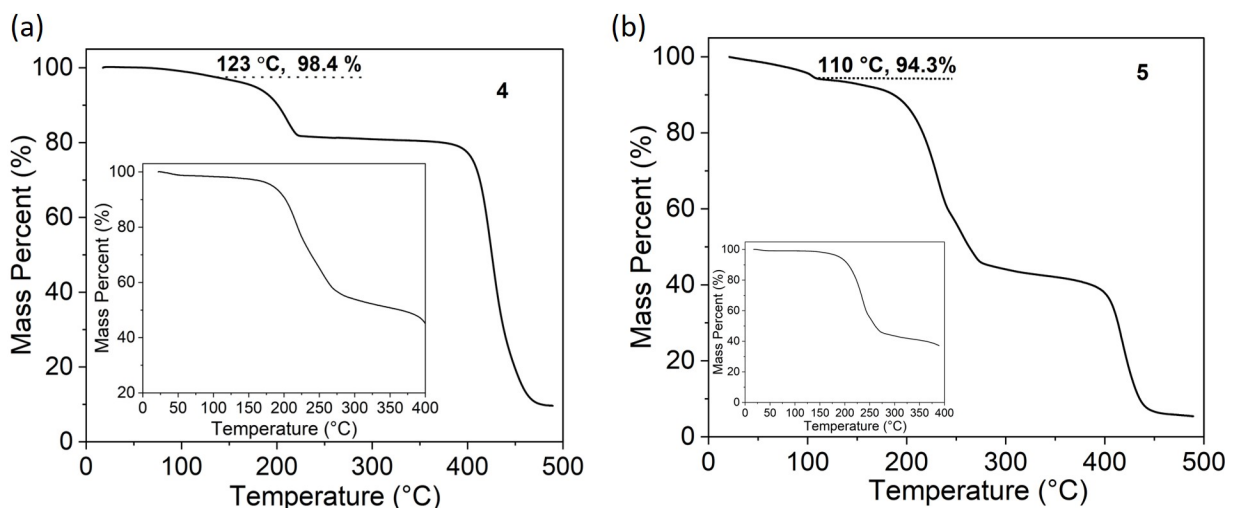


**Figure S2.** Thermogravimetric curves of **4** and **5** and their desolvated forms (insets). The mass loss of 1.6% reached at 123 °C for **4** and 5.7% reached at 110 °C for **5** corresponds to the loss of ~0.5 Me<sub>2</sub>CO molecule and ~2 MeCN molecules per formula unit, respectively.

**Table S1.** Data collection and crystal structure refinement parameters for **1**·5*MeCN*, **2**·3*MeCN*, and **2**.

Formula	FeC <sub>68</sub> N <sub>27</sub> H <sub>45</sub> ( <b>1</b> ·5 <i>MeCN</i> )		FeC <sub>52</sub> N <sub>21</sub> H <sub>35</sub> ( <b>2</b> ·3 <i>MeCN</i> )		FeC <sub>46</sub> N <sub>18</sub> H <sub>26</sub> ( <b>2</b> )		
<i>T</i> , K	90(1)	250(1)	90(1)	250(1)	90(1)	100(1)	250(1)
CCDC number	2085716	2085556	2085554	2085557	2085553	2085555	2085812
Formula weight	1296.16	1296.16	1009.86	1009.86	886.70	886.70	886.70
Space group	<i>P</i> 1̄	<i>P</i> 1̄	<i>P</i> 2 <sub>1</sub> /n	<i>P</i> 2 <sub>1</sub> /n	<i>P</i> 2 <sub>1</sub> /n	<i>P</i> 2 <sub>1</sub> /n	<i>P</i> 2 <sub>1</sub> /n
<i>a</i> , Å	7.7762(2)	7.8497(1)	18.0520(2)	18.3634(2)	17.0540(5)	17.0726(5)	17.3168(7)
<i>b</i> , Å	13.5083(3)	13.8050(2)	8.3187(1)	8.4220(1)	8.4678(4)	8.4731(3)	8.6392(3)
<i>c</i> , Å	31.1622(5)	31.8342(4)	33.6006(3)	33.4443(3)	28.8259(13)	28.8012(12)	28.4775(14)
$\alpha$ , deg	81.958(2)	99.377(1)	90	90	90	90	90
$\beta$ , deg	89.256(2)	90.383(1)	103.229(1)	102.637(1)	92.364(4)	92.371(3)	92.662(4)
$\gamma$ , deg	88.883(2)	92.564(1)	90	90	90	90	90
<i>V</i> , Å <sup>3</sup>	3240.40(12)	3399.87(8)	4911.9(9)	5047.1(1)	4159.2(3)	4162.8(3)	4255.7(3)
<i>Z</i>	2	2	4	4	4	4	4
Crystal color	dark green	dark green	dark green	dark green	dark green	dark green	dark green
Crystal size, mm <sup>3</sup>	0.56×0.48×0.23	0.51×0.20×0.17	0.61×0.41×0.27	0.61×0.41×0.27	0.18×0.15×0.10	0.18×0.15×0.10	0.42×0.31×0.20
<i>d</i> <sub>calc</sub> , g/cm <sup>3</sup>	1.328	1.245	1.366	1.329	1.416	1.415	1.373
$\mu$ , mm <sup>-1</sup>	2.396	2.273	2.959	2.879	3.392	3.389	3.291
$\lambda$ , Å	1.54184	1.54184	1.54184	1.54184	1.54184	1.54184	1.54184
2θ <sub>max</sub> , deg	77.65	72.96	76.50	76.34	66.02	62.42	74.10
Total reflections	23357	44556	34787	36485	6778	18522	7534
<i>R</i> <sub>int</sub>	0.032	0.034	0.030	0.024	0.042	0.047	0.068
Unique reflections	11686	13071	9935	10230	4286	6854	
Parameters refined	866	854	671	670	586	586	587
Restraints used	9	6	0	0	0	0	0
<i>R</i> <sub>1</sub> , <i>wR</i> <sub>2</sub> [ <i>I</i> > 2σ( <i>I</i> )] <sup>a</sup>	0.075, 0.217	0.079, 0.245	0.047, 0.104	0.042, 0.101	0.064, 0.159	0.063, 0.149	0.063, 0.172
<i>R</i> <sub>1</sub> , <i>wR</i> <sub>2</sub> (all data)	0.083, 0.226	0.090, 0.258	0.047, 0.101	0.049, 0.104	0.110, 0.185	0.100, 0.173	0.089, 0.189
Goodness of fit <sup>b</sup>	1.049	1.023	1.043	1.110	1.019	1.019	1.036
Diff. peak/hole, e/Å <sup>3</sup>	0.75, -0.43	0.65, -0.32	0.53, -0.71	0.28, -0.32	0.58, -0.39	0.48, -0.25	0.42, -0.54

<sup>a</sup>  $R_1 = \sum ||F_o|| - |F_c| | / \sum |F_o|$ ;  $wR_2 = [\sum [w(F_o^2 - F_c^2)^2] / \sum [w(F_o^2)^2]]^{1/2}$ ;

<sup>b</sup> Goodness-of-fit =  $[\sum [w(F_o^2 - F_c^2)^2] / (N_{\text{obs}} - N_{\text{params}})]^{1/2}$ , based on all data.

**Table S2.** Data collection and crystal structure refinement parameters for **4** and **5**.

Formula	FeC <sub>64</sub> N <sub>24</sub> O <sub>2</sub> H <sub>29</sub> ( <b>3</b> ) <sup>*</sup>	FeC <sub>92</sub> N <sub>26</sub> O <sub>2</sub> H <sub>54</sub> ( <b>4</b> )	FeC <sub>70</sub> N <sub>26</sub> H <sub>34</sub> ( <b>5</b> )
T, K	100(2)	250(2)	250(2)
CCDC number	2085559	2085558	2085560
Formula weight	1189.96	1611.46	1597.40
Space group	C2/c	P $\bar{1}$	P $\bar{1}$
a, Å	10.3372(5)	10.0233(6)	9.9579(1)
b, Å	19.2020(8)	10.1699(6)	22.3384(2)
c, Å	19.2720(5)	39.5589(9)	23.3617(2)
$\alpha$ , deg	68.570(4)	86.567(3)	114.800(10)
$\beta$ , deg	81.877(4)	85.517(3)	90.3930(10)
$\gamma$ , deg	83.090(4)	88.337(5)	97.8690(10)
V, Å <sup>3</sup>	3515.4(3)	4011.7(4)	4661.3(8)
Z	2	2	2
Crystal color	black	dark green	dark green
Crystal size, mm <sup>3</sup>	0.46×0.19×0.06	0.33×0.18×0.09	0.29×0.09×0.07
$d_{\text{calc}}$ , g/cm <sup>3</sup>	1.127	1.321	1.138
$\mu$ , mm <sup>-1</sup>	2.158	2.044	1.765
$\lambda$ , Å	1.54184	1.54184	1.54184
2 $\theta_{\text{max}}$ , deg	76.13	72.70	71.97
Total reflections	39203	12402	27959
$R_{\text{int}}$	0.069	0.089	0.041
Unique reflections	13877	9980	17886
Parameters refined	717	1094	1091
Restraints used	4	0	0
$R_1$ , $wR_2$ [ $I > 2\sigma(I)$ ] <sup>a</sup>	0.219, 0.495	0.055, 0.078	0.056, 0.146
$R_1$ , $wR_2$ (all data)	0.239, 0.518	0.039, 0.066	0.067, 0.153
Goodness of fit <sup>b</sup>	2.206	1.076	1.073
Diff. peak/hole, e/Å <sup>3</sup>	8.15, -1.68	0.30, -0.40	0.51, -0.57

<sup>a</sup>  $R_1 = \sum ||F_o| - |F_c|| / \sum |F_o|$ ;  $wR_2 = [\sum [w(F_o^2 - F_c^2)^2] / \sum [w(F_o^2)^2]]^{1/2}$ ;

<sup>b</sup> Goodness-of-fit =  $[\sum [w(F_o^2 - F_c^2)^2] / (N_{\text{obs}} - N_{\text{params}})]^{1/2}$ , based on all data.

\* Due to the extremely poor quality of diffraction of crystals of complex **3**, only an approximate structural model has been achieved, with the use of the solvent mask as implemented in the Olex2 software.

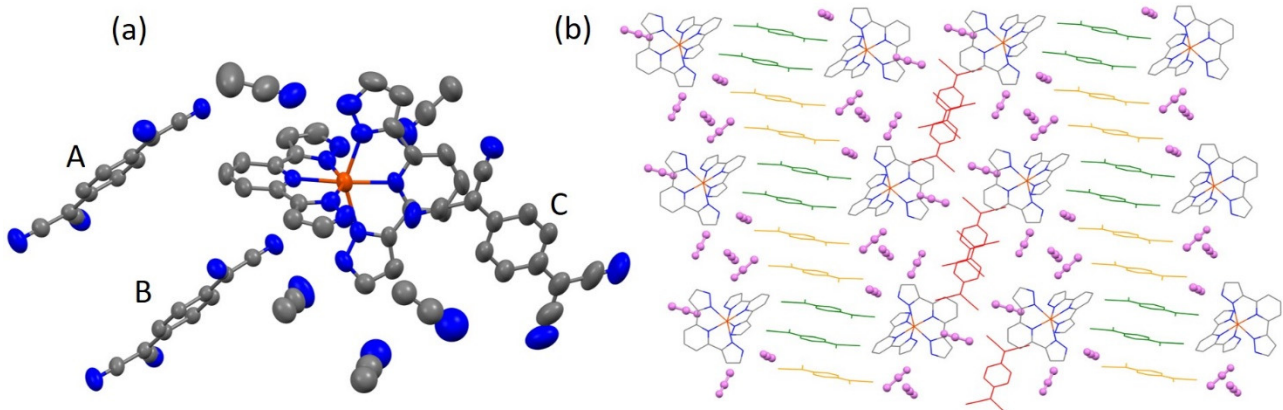


**Figure S4.** The asymmetric unit (a) and crystal packing (b) of **1·5MeCN**. In panel (a), the thermal ellipsoids are at the 50% probability level. In panel (b), the interstitial solvent molecules are emphasized with pink color, while the crystallographically distinct TCNQ units are indicated with yellow, green, and red (see the main text for a detailed description). Color scheme for other atoms: Fe = orange, N = blue, C = gray. The H atoms are omitted for clarity.

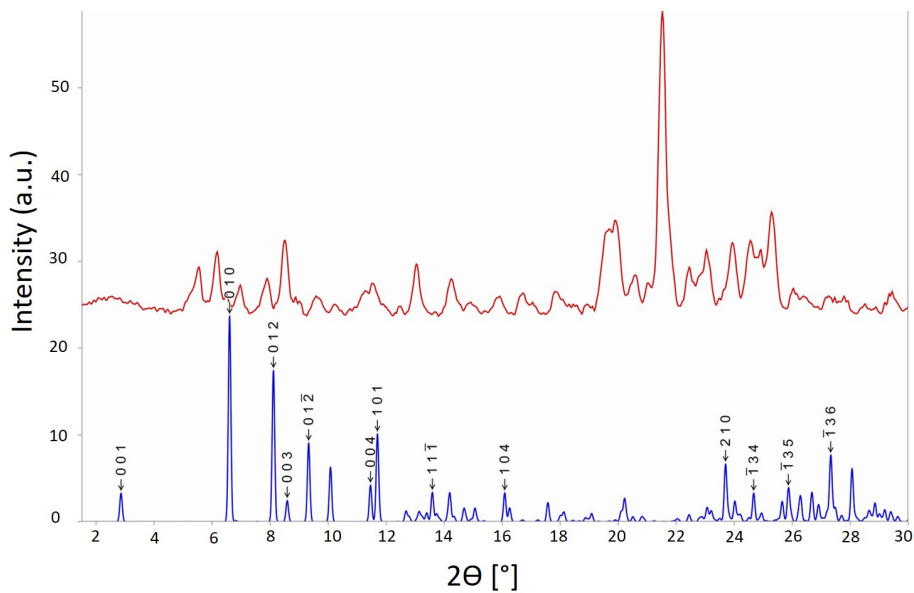


**Figure S3.** Powder X-ray diffraction pattern of **1** obtained by desolvation of **1·5MeCN** (top) and the calculated powder X-ray diffraction pattern of **1·5MeCN** (bottom).

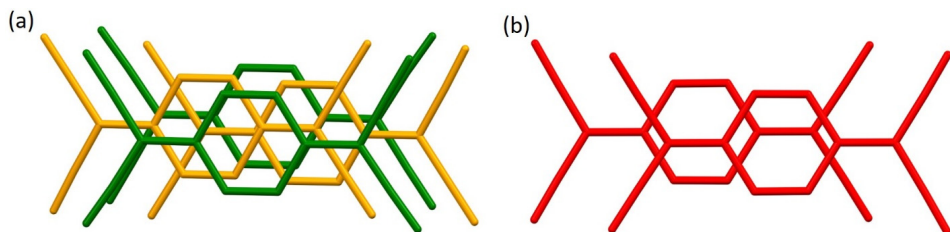
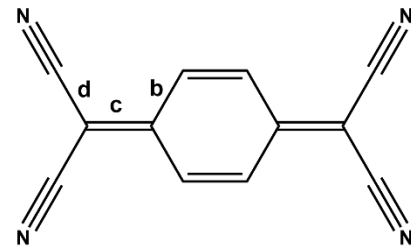


**Figure S5.** The overlap modes of TCNQ units in **1·5MeCN**: (a) the ring-over-ring in  $\text{TCNQ}^{\text{A}}-\text{TCNQ}^{\text{B}}$  and ring-over-external-bond in  $\text{TCNQ}^{\text{A}}-\text{TCNQ}^{\text{A}}$  and  $\text{TCNQ}^{\text{B}}-\text{TCNQ}^{\text{B}}$ ; (b) the ring-over-external-bond in  $\text{TCNQ}^{\text{C}}-\text{TCNQ}^{\text{C}}$ .

**Table S3.** The calculation of charges ( $-\delta$ ) for four different  $\text{TCNQ}^{\delta^-}$  species in the crystal structures of **1·5MeCN**, **2·3MeCN**, and **2** determined at 250 K. The charges were estimated from the empirical Kistenmacher relationship [T.J. Kistenmacher, *et al.* Acta Crystallogr. Sect. B, B38 (1982) 1193–1199] and scaled to make the total absolute charge on the  $\text{TCNQ}^{\delta^-}$  anions equal to the total charge of the cations.



$$-\delta = -41.67[c/(b+d)] + 19.83$$

TCNQ unit <sup>a</sup>	b, Å	c, Å	d, Å	c/(b+d)*	−δ(calcd.)	−δ(scaled)
$\text{TCNQ}^0$	1.448	1.374	1.440	0.476	0.0	n/a
$\text{TCNQ}^{1^-}$	1.423	1.420	1.416	0.500	-1.0	
$\text{TCNQ}^{0.5^-}$	1.434	1.396	1.428	0.488	-0.50	
<b>1·5MeCN-TCNQ<sup>A</sup></b>	1.432	1.399	1.424	0.489	-0.57	-0.58
<b>1·5MeCN-TCNQ<sup>B</sup></b>	1.435	1.390	1.427	0.486	-0.41	-0.41
<b>1·3MeCN-TCNQ<sup>C</sup></b>	1.418	1.412	1.406	0.500	-1.01	-1.01
<b>2·3MeCN-TCNQ<sup>A</sup></b>	1.414	1.426	1.410	0.505	-1.22	-1.08
<b>2·3MeCN-TCNQ<sup>B</sup></b>	1.421	1.420	1.415	0.500	-1.03	-0.92
<b>2-TCNQ<sup>A</sup></b>	1.417	1.422	1.414	0.502	-1.09	-1.08
<b>2-TCNQ<sup>B</sup></b>	1.424	1.414	1.415	1.498	-0.93	-0.92

<sup>a</sup> The metric parameters for  $\text{TCNQ}^0$ ,  $\text{TCNQ}^{1^-}$ , and  $\text{TCNQ}^{0.5^-}$  have been taken from the reference given in the caption.

**Table S4.** The calculation of charges ( $-\delta$ ) for four different  $\text{TCNQ}^{\delta^-}$  species in the crystal structures **4** and **5** determined at 300 K. The charges were estimated from the empirical Kistenmacher relationship and scaled to make the total absolute charge on the  $\text{TCNQ}^{\delta^-}$  anions equal to the total charge of the cations.

TCNQ unit	b, Å	c, Å	d, Å	c/(b+d)	−δ(calcd.)	−δ(scaled)
<b>4-TCNQ<sup>A</sup></b>	1.419	1.427	1.412	0.504	-1.18	-0.70
<b>4-TCNQ<sup>B</sup></b>	1.428	1.389	1.422	0.487	-0.48	-0.28
<b>4-TCNQ<sup>C</sup></b>	1.436	1.388	1.429	0.485	-0.36	-0.21
<b>4-TCNQ<sup>A'</sup></b>	1.423	1.406	1.419	0.495	-0.79	-0.47
<b>4-TCNQ<sup>B'</sup></b>	1.429	1.398	1.423	0.490	-0.60	-0.36
<b>4-TCNQ<sup>C'</sup></b>	1.439	1.367	1.437	0.476	0.02	0.02
<b>5-TCNQ<sup>A</sup></b>	1.433	1.393	1.427	0.487	-0.46	-0.40
<b>5-TCNQ<sup>B</sup></b>	1.427	1.406	1.424	0.493	-0.72	-0.62
<b>5-TCNQ<sup>C</sup></b>	1.424	1.417	1.418	0.499	-0.95	-0.82
<b>5-TCNQ<sup>A'</sup></b>	1.438	1.379	1.431	0.481	-0.20	-0.16
<b>5-TCNQ<sup>B'</sup></b>	1.451	1.371	1.431	0.476	0.01	0.01

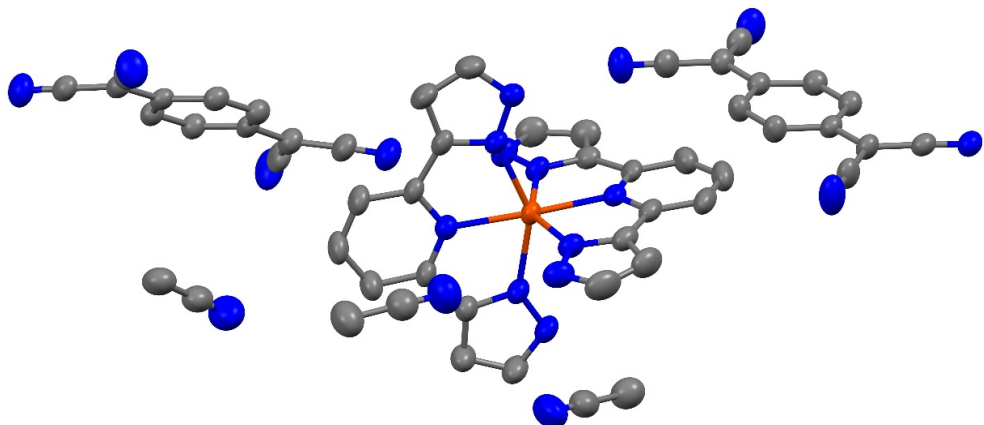


**Figure S6.** The asymmetric unit of **2·3MeCN**. Color scheme: Fe = orange, N = blue, C = gray. The H atoms are omitted for clarity. The thermal ellipsoids are at the 50% probability level.

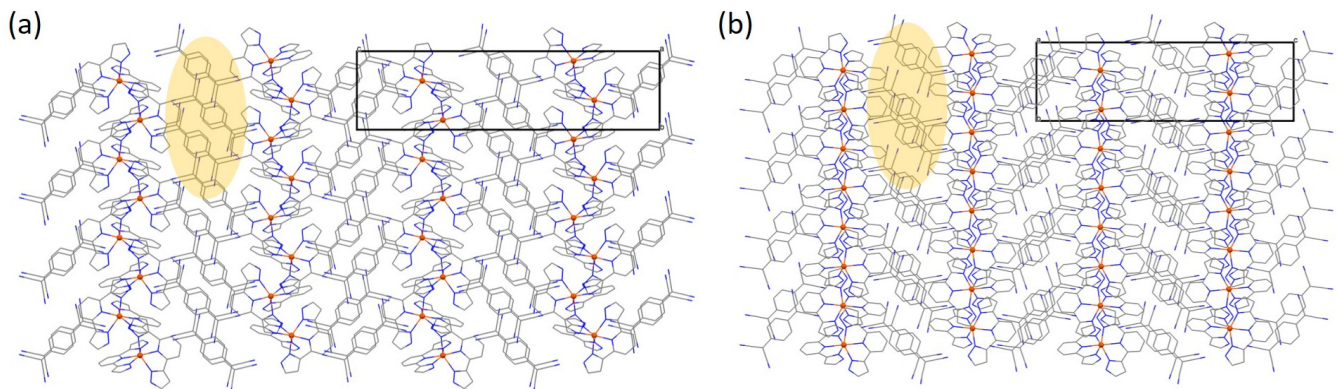


**Figure S7.** The crystal packing of **2·3MeCN** (a) and **2** (b) viewed down the stacks of  $(\text{TCNQ})^{2-}$  dimers. The closer approach of the cations and anions upon the loss of interstitial solvent is obvious.

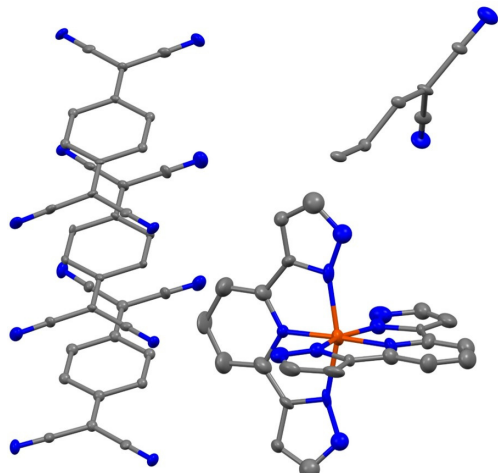


**Figure S8.** The asymmetric unit of **3**. Color scheme: Fe = orange, N = blue, C = gray. The H atoms are omitted for clarity. The contribution to X-ray diffraction intensities from the severely disordered solvent molecules was eliminated by the solvent-mask procedure. The thermal ellipsoids are at the 50% probability level.

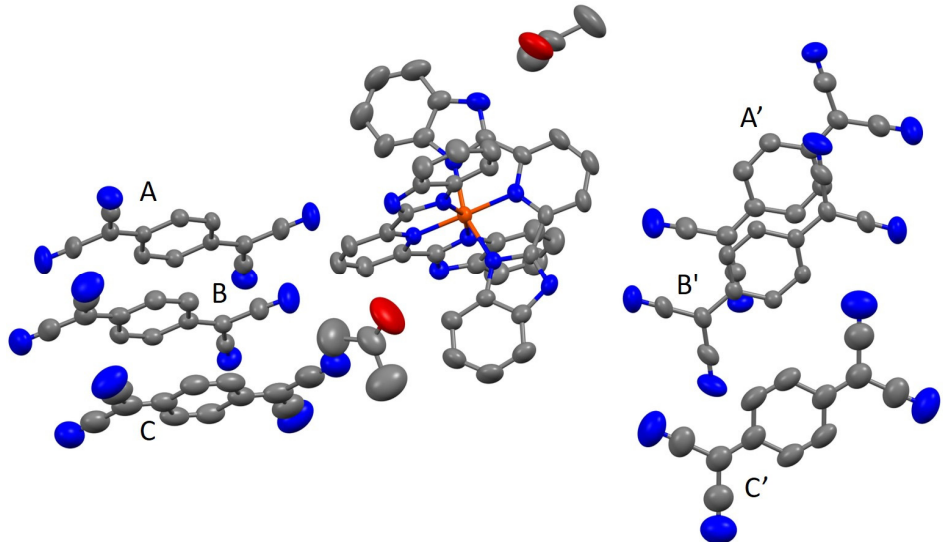


**Figure S9.** The asymmetric unit of **4**. Color scheme: Fe = orange, O = red, N = blue, C = gray. The H atoms are omitted for clarity. The thermal ellipsoids are at the 50% probability level.

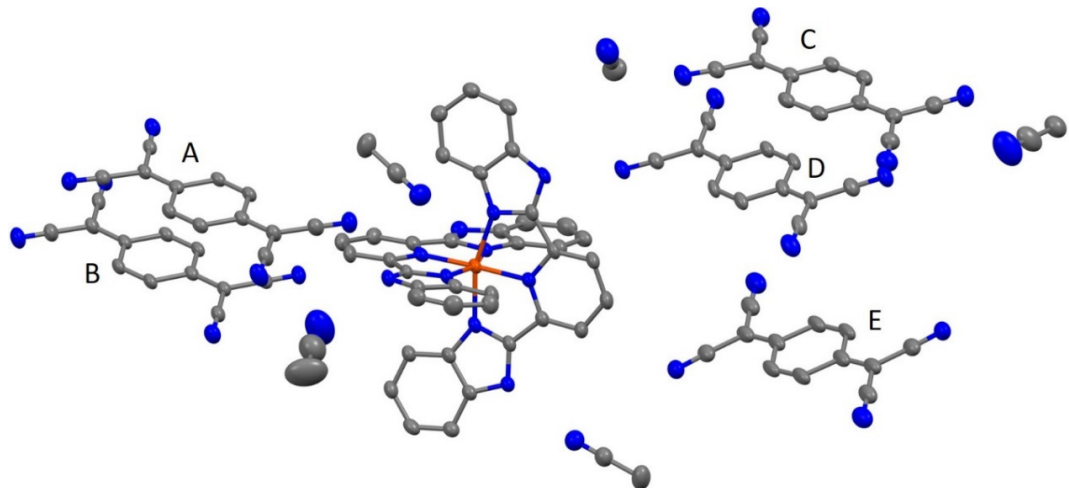


**Figure S10.** The asymmetric unit of **5**. Color scheme: Fe = orange, O = red, N = blue, C = gray. The H atoms are omitted for clarity. The thermal ellipsoids are at the 50% probability level.

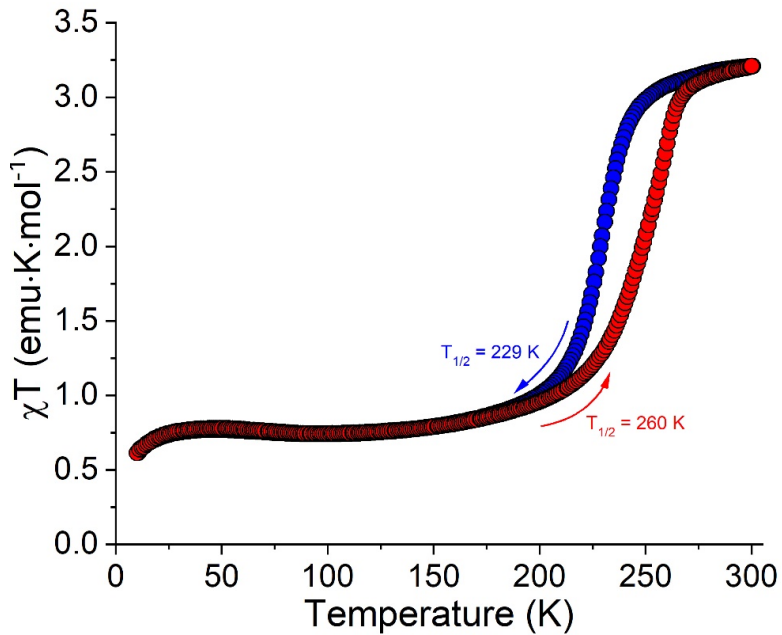


**Figure S11.** The temperature dependence of  $\chi T$  measured on the sample of 1.5MeCN kept in the magnetometer chamber at 300 K for 1 h prior to the measurement. The measurement was performed first in the cooling mode from 300 to 5 K and then in the warming mode from 5 to 300 K, at the rate of 1 K/min.

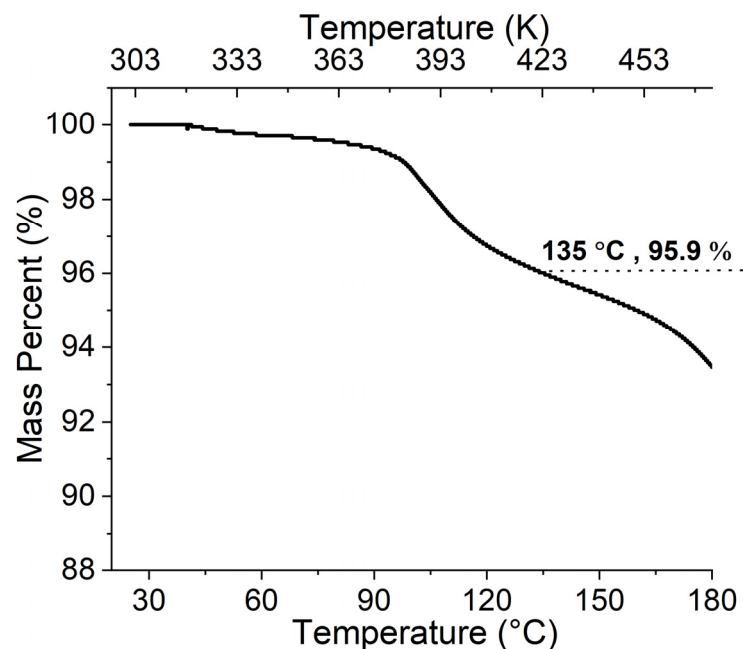


**Figure S12.** Thermogravimetric curve of the sample 1.5MeCN subjected to two consecutive cooling-heating measurement cycles between 350 and 5 K, at 1 K/min, inside the magnetometer chamber. Upon completion of the second cycle, the sample was cooled to 300 K at 10 K/min, removed from the magnetometer, and immediately subjected to TGA. The mass loss of 4.1% reached at the inflection point at 135 °C corresponds to the loss of ~1 MeCN molecule per formula unit (calculated – 3.63%).

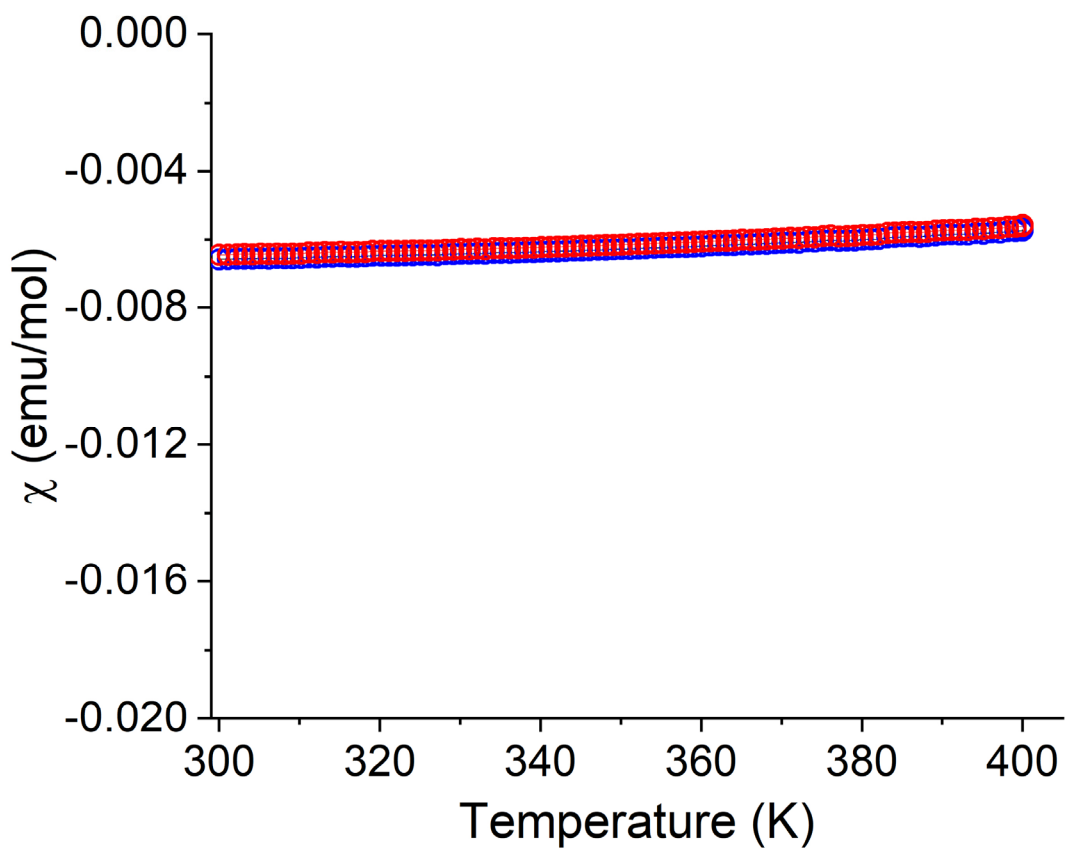


**Figure S13.** Temperature dependence of  $\chi$  measured for samples 4 (blue) and 5 (red) between 300 and 400 K.